Toxicon:X 8 (2020) 100060

Contents lists available at ScienceDirect

Toxicon: X

journal homepage: www.journals.elsevier.com/toxicon-x

Global transcriptomic profiling of microcystin-LR or -RR treated hepatocytes (HepaRG)

Adam D. Biales [a,*], David C. Bencic [a], Robert W. Flick [a], Armah Delacruz [a], Denise A. Gordon [a], Weichun Huang [b]

[a] U.S. Environmental Protection Agency, Office of Research and Development, Cincinnati, OH, 45268, USA
[b] U.S. Environmental Protection Agency, Office of Research and Development, Research Triangle Park, NC, 27709, USA

ARTICLE INFO

Keywords:
Microcystin-LR
Microcystin-RR
RNA-seq
Transcriptomics
ER stress
Oxidative stress
Hepatocytes
MC-LR
MC-RR
Gene expression

ABSTRACT

The canonical mode of action (MOA) of microcystins (MC) is the inhibition of protein phosphatases, but complete characterization of toxicity pathways is lacking. The existence of over 200 MC congeners complicates risk estimates worldwide. This work employed RNA-seq to provide an unbiased and comprehensive characterization of cellular targets and impacted cellular processes of hepatocytes exposed to either MC-LR or MC-RR congeners. The human hepatocyte cell line, HepaRG, was treated with three concentrations of MC-LR or -RR for 2 h. Significant reduction in cell survival was observed in LR1000 and LR100 treatments whereas no acute toxicity was observed in any MR-RR treatment. RNA-seq was performed on all treatments of MC-LR and -RR. Differentially expressed genes and pathways associated with oxidative and endoplasmic reticulum (ER) stress, and the unfolded protein response (UPR) were highly enriched by both congeners as were inflammatory pathways. Genes associated with both apoptotic and inflammatory pathways were enriched in LR1000. We present a model of MC toxicity that immediately causes oxidative stress and leads to ER stress and the activation of the UPR. Differential activation of the three arms of the UPR and the kinetics of JNK activation ultimately determine whether cell survival or apoptosis is favored. Extracellular exosomes were enrichment of by both congeners, suggesting a previously unidentified mechanism for MC-dependent extracellular signaling. The complement system was enriched only in MC-RR treatments, suggesting congener-specific differences in cellular effects. This study provided an unbiased snapshot of the early systemic hepatocyte response to MC-LR and MC-RR congeners and may explain differences in toxicity among MC congeners.

1. Introduction

Microcystins (MCs) are hepatotoxic heptapeptides produced by numerous cyanobacteria species. Though MC toxicity is generally associated with hepatotoxicity(Yoshida et al., 1998), effects have also been observed in other tissues (Alverca et al., 2009; Lin et al., 2016). Human exposure is primarily through oral ingestion (Massey et al., 2018). MCs are then absorbed through the small intestines, travel via the hepatic portal system and accumulate in the liver. There are at least 279 congeners of microcystins that differ in their structure and toxicity (Bouaicha et al., 2019) and these often occur as mixtures in blooms (Graham et al., 2010). Congeners mostly differ by substitutions of L-amino acid at positions two and four (Harke et al., 2016). Due to their size and hydrophilic nature, most MC congeners require active transport through the organic anion transport proteins (OATP) (Fischer et al., 2005; Runnegar et al., 1995). However, more hydrophobic variants can potentially enter cells via direct diffusion across the cellular membrane (Vesterkvist and Meriluoto, 2003). Microcystin-LR (MC-LR) is the most common, well studied, and among the most toxic MC congeners. Less is known about microcystin-RR (MC-RR) which is also commonly found in cyanobacteria blooms (Diez-Quijada et al., 2019; Dyble et al., 2008) and co-occurs with MC-LR (Graham et al., 2010). MC-LR has a leucine and an arginine in the variable positions, while MC-RR has two arginines, resulting in hydrophobicity and toxicokinetic differences (Vesterkvist and Meriluoto, 2003).

Though the MCs have been shown to have multiple intracellular effects, their canonical intracellular mode of action (MOA) is the inhibition of protein phosphatases (PP) 1 and 2A (Yoshizawa et al., 1990). PP inhibition causes hyperphosphorylation of cellular proteins, including cytoskeletal proteins, resulting in disruption of the cytoskeletal architecture, a loss of cellular integrity (Batista et al., 2003),

* Corresponding author. 26 W. Martin Luther King Dr, Cincinnati, OH, 45268, USA.
E-mail address: Biales.adam@epa.gov (A.D. Biales).

https://doi.org/10.1016/j.toxcx.2020.100060
Received 10 August 2020; Received in revised form 24 September 2020; Accepted 27 September 2020
Available online 7 October 2020

Abbreviations

AhR	aryl hydrocarbon receptor
AP-1	activator protein 1
APR	acute phase response
ARE	antioxidant response element
ATF3	activating transcription factor 3
ATF6	activating transcription factor 6
BWA	Burrows-Wheeler Aligner
CHOP	C/EBP homologous protein; DDIT3 damage inducible transcript 3
CPE	cytopathic effects
DAVID	Database for Annotation, Visualization and Integrated Discovery
DEG	differentially expressed genes
DR	death receptor
ER	endoplasmic reticulum
ERK	extracellular signal-regulated kinase
FDR	false discovery rate
FOS	fos proto-oncogene, AP-1 transcription factor subunit
FXR	farnesoid x receptor
GADD34	growth arrest and DNA damage-inducible protein 34
GCLC	Glutamate-Cysteine Ligase Catalytic Subunit
GCLM	Glutamate-Cysteine Ligase Modifier Subunit
GEO	Gene Expression Omnibus
GO	gene ontology
GPX	glutathione peroxidase
HAB	harmful algal blooms
HBSS	Hanks balanced salt solution
IPA	Ingenuity Pathway Analysis
IRE-1	Inositol-requiring enzyme 1
JNK	c-jun N-terminal kinase
JUN	transcription factor AP-1
MAPK	mitogen activated protein kinase
MC	microcystin
MOA	mode of action
NCBI	National Center for Biotechnology Information
NF-κβ	nuclear factor kappa beta
NOXA/PMAIP1	Phorbol-12-myristate-13-acetate-induced protein 1
Nrf-2	nuclear factor erythroid 2-related factor 2
OATP	organic anion transport proteins
PERK	Protein Kinase R-like *ER* Kinase
PP	protein phosphatase
PPAR	peroxisome proliferator-activated receptor
PUMA	p53 up-regulated modulator of apoptosis
ROS	reactive oxygen species
RTA	Real Time Analysis
SVA	Surrogate Variable Analysis
UPR	unfolded protein response
XTT	2,3-bis-(2-methoxy-4-nitro-5-sulfophenyl)-2H-tetrazolium-5-carboxanilide

intrahepatic hemorrhaging and eventual death (Yoshida et al., 1998). MC-LR and -RR have been shown to have similar inhibitory effects on PP1 and PP2a (Fischer et al., 2010; Hoeger et al., 2007), yet they differ by an order of magnitude in acute toxicity (Gupta et al., 2003). This is at least partially explained by toxicokinetic differences (Fischer et al., 2010); however, recent experimental evidence suggests that MC-LR may have molecular targets outside of PP1 and PP2A (Chen et al., 2006; Pereira et al., 2013) suggesting the possibility that cellular targets may differ among MC congeners.

Many cellular responses to MC exposure are dependent on the *de novo* production of proteins resulting from differential expression of genes(Takumi et al., 2010). In order to better understand the molecular mechanisms underlying cellular responses, several studies have measured MC-dependent changes in gene expression. For the most part, expression-based studies have been conducted using MC-LR and have targeted pathway-specific genes or proteins as indicators of perturbation (Christen et al., 2013). Collectively, these studies have identified several affected pathways; however, as these studies were conducted in different model systems with different exposure parameters, a holistic picture of the transcriptional response to MC-LR is still lacking. Fewer studies have attempted to characterize the transcriptional response and intracellular effects induced by MC-RR. MC-LR and -RR often co-occur and their cellular targets, outside of PP inhibition, may differ, leading to uncertainty in the risk posed by mixture exposures. Thus, there is a need for a more comprehensive characterization of their individual cellular targets and effects. The objective of the current work is to characterize the transcriptional response of a human hepatocyte cell line (HepaRG) to MC-LR and -RR. HepaRG cells were selected because they retain intact liver functions, express a number of cytochrome P450 and nuclear receptors, as well as microcystin-associated transporters (OATP1B1 and OATP1B3), and respond similarly to human primary hepatocytes upon toxicant challenge (Higuchi et al., 2014; Josse et al., 2008; Szabo et al., 2013). RNA-seq was used to provide an unsupervised evaluation of global gene expression in cells exposed to three concentrations of either MC-LR or -RR. This approach provides a means to substantiate existing targeted experimental evidence, find potential linkages among affected cellular processes, and identify new potential MOA and intracellular targets.

2. Material and methods

2.1. Cell culture and exposures

Four independent exposure experiments were conducted. In order to maximize replicate number within each treatment group, all individual replicates from a given treatment group were used for gene expression analysis. The number of replicates used in gene expression by experiment is defined in Table 1. Using replicates across experiments incorporated technical and batch variability resulting from different cell and MC lot numbers, RNA isolation, library development, and sequencing runs.

Differentiated HepaRG (Life Technologies, Carlsbad, CA, USA) were thawed in HepaRG in Working Medium (WM; Williams' medium E supplemented with glutamine and HepaRG thaw, plate and general-purpose medium supplement) according to the manufacturer's procedure (Life Technologies). Cells were resuspended in WM and cell viability was determined by Trypan Blue dye exclusion; cell suspensions were >85% viable.

Cells were seeded at 5×10^5 cells/well onto a pre-wetted sterile flat-

Table 1
Number and direction of statistically significant DEGs (FDR < 0.05) and replicate number per experimental batch and treatment group.

Group	Total	Up-regulated	Down-regulated	Experiment N				N total
				1	2	3	4	
LR10	339	230	109	2	6	6	5	*19*
LR100	171	116	55	5	6	6	5	*22*
LR1000	2098	1740	358	5	6	6	1	*18*
RR10	12	11	1	3	6	0	4	*13*
RR100	1255	1130	125	4	6	6	6	*22*
RR1000	1279	1138	141	4	6	6	2	*18*
Solvent				9	12	6	9	*36*

bottom collagen coated 24-well plate (Life Technologies) and incubated overnight. WM was replaced with pre-warmed HepaRG Toxicity Working Medium (TM; Williams' medium E supplemented with glutamine and HepaRG toxicity medium supplement) and re-incubated until MC exposure on day 7.

MCs (MC-LR or -RR; Calbiochem, La Jolla, CA, USA) were diluted in TM and used on the same day. Cells were exposed with 10, 100 and 1000 ng mL^{-1} of MC-LR or MC-RR, or to solvent (1% methanol) in replicates for 2 h in a humidified 5% CO_2, 37 °C incubator. Cells were harvested and washed with 1 mL Hank's Balanced Salt Solution (HBSS; Thermo Fisher Scientific, Waltham, MA, USA), lysed in QIAzol ™ Lysis Reagent (Qiagen, Germantown, MD, USA), and stored at −80 °C until RNA isolation.

2.2. Cell cytotoxicity

In vitro cell cytotoxicity was assessed microscopically and biochemically. Cells exhibit cytopathic effects (CPE) prior to apoptosis and at subcytotoxic concentrations, suggesting microscopic examination is more sensitive; however, it yields only observational results. Cells were seeded at 4×10^4 cells/well onto a pre-wetted sterile flat-bottom collagen coated 96-well plate and cultured under a humidified environment at 37 °C overnight and treated as described above. Cells were exposed with 10, 100 and 1000 ng mL^{-1} MC-LR or MC-RR (same lot used within 24-well plates). At 6 h post exposure to MCs, cells were examined for CPEs (cell rounding, swelling/enlarging, clumping/grouping, rounding, blebbing, detaching, having refractile and amorphous shape, increased granularity, and enlarged ghost cells).

Following 48 h of further incubation, cells (control, n = 15; MC samples, n = 5) were washed with pre-warmed HBSS 5X. After the addition of activated XTT substrate (XTT Cell Proliferation Assay, ATCC, Manassas, VA, USA), the plate was incubated for 4 h and mixed. Optical density was determined using a spectrophotometer (Molecular Devices SpectraMax M2, Sunnyvale, CA, USA). A linear mixed effects model (lme4 v 1.1–19 (Bates et al., 2015)) with experiment as a random effect was performed in R (Team, 2017) to determine statistical significance ($p < 0.05$); p values were obtained using the lmerTest package (Kuznetsova et al., 2017).

2.3. RNA isolation

Cells were thawed in Qiazol lysis buffer (Qiagen, Hilden, DE) and further homogenized (Bullet Blender Storm 24 mixer mill, Next Advance, Averill Park, NY, USA) using the manufacturer's recommended settings. Approximately 250 μl of chloroform:isoamyl alcohol (24:1; Sigma-Aldrich Chemical Co., St. Louis, MO, USA) was added to each tube, mixed by inversion, and vortexed and incubated at room temperature for 3 min and transferred to a 1.5 ml Heavy Phase Lock Gel microfuge tube (5Prime, Inc., Gaithersburg, MD, USA), incubated on ice (10 min) and centrifuged at 14,200 *g* (5 min, room temperature (RT)). The supernatant was transferred to a microcentrifuge tube (Eppendorf North America, Hauppauge, NY, USA) and mixed with an equal volume of 70% ethanol and put on a RNeasy® MinElute Clean Up kit 2.0 ml column (Qiagen) and processed according to the manufacturer's protocol with DNase treatment (RNase-free DNase kit, Qiagen) prior to final cleanup and elution. RNA was quantified and quality was confirmed using an Agilent RNA 6000 Nano kit with a 2100 Bioanalyzer (Agilent Technologies, Inc., Wilmington, DE). Typical RIN scores were above 9. RNA eluates were stored at −80 °C.

2.4. Library preparation and sequencing

Sequencing libraries were prepared using the TruSeq Stranded mRNA Library Prep for NeoPrep kit (Illumina, San Diego, CA, USA), following the manufacturer's protocol. An input of 100 ng total RNA was used for each sample. Additional resuspension buffer was added to each library to obtain a final total volume of about 24 μL. The concentration of each library was determined using either the KAPA Library Quantification Kit for Illumina Platforms (Kapa Biosystems) or the Qubit dsDNA HS Assay kit (Thermo Fisher Scientific). Libraries were normalized to 10 nM and combined into pools of 8–16 samples. Dilutions of libraries for quantitation and pooling was done using 10 mM Tris-HCl, pH 8.5.

Prior to sequencing at Michigan State University Research Technology Support Facility (MSU), the quality and quantity of library pools were determined by MSU using a combination of Qubit dsDNA HS, either Caliper LabChipGX HS DNA or Agilent Bioanalyzer High Sensitivity DNA and the Kapa Illumina Library Quantification qPCR assays. Each pool was loaded onto one lane of an Illumina HiSeq 4000 flow cell and sequencing performed in a 1 × 50bp single read format using HiSeq 4000 SBS reagents. Base calling was done by Illumina Real Time Analysis (RTA) v2.7.7 and output of RTA was demultiplexed and converted to FastQ format with Illumina Bcl2fastq v2.19.1.

2.5. RNA-seq data analysis

Raw sequencing data were quality checked, using FastQC (Brown et al., 2017) for read quality, GC content, presence of adaptors, over-represented k-mers and duplicated reads derived from sequencing issues, PCR bias, or contaminations. Reads then were mapped, using BWA (Li and Durbin, 2009), to the human genome transcript references (GRCh38) from the GENCODE (Harrow et al., 2012). GENCODE comprehensive gene set was used for this analysis as it has more exons, greater genomic coverage and more transcript variants than the NCBI RefSeq in both genome and exome datasets (Frankish et al., 2015). Our in-house RNA-seq analysis pipeline based on the improved version of EpiCenter (Huang et al., 2011) was then used to quantify abundance levels of individual transcripts and identification of DEGs. Read count data were normalized so that the average number of total mapped reads was the same for all replicates across all groups. The SVA package (Leek et al., 2018) was used to remove batch effects before differential gene expression analysis. To remove batch effects from the four different experiments, we first filtered out lowly expressed transcripts with normalized read count <50 in all individual groups. We then converted discrete read count data into continuous data by log2 transformation. To deal with potential zero count data issue, we added 1 to the normalized counts before taking the log2 transformation. We then use the ComBat function from the SVA package to remove batch effect. The batch-removed data from ComBat were then converted back to discrete read count data by the inverse log2 function, i.e., the exponential function. All sequencing and meta data have been deposited in the NCBI GEO database (GSE147999O). A 5% false discovery rate (FDR) was used to as the cutoff for statistically significant transcripts. Functional annotation and enrichment analysis of DEG lists was conducted using both the Database for Annotation, Visualization and Integrated Discovery (DAVID) v6.8 (Huang da et al., 2009) and Ingenuity Pathway Analysis (IPA; QIAGEN Inc., https://www.qiagenbioinformatics.com/products/ingenuitypathway-analysis). An FDR cutoff of 0.05 was used to determine significance. Due to the unusually high replicate number, the fact that biological relevance does not track with the magnitude of expression (Evans, 2015; St Laurent et al., 2013), and to better fulfill the stated objectives of the study to identify genes, pathways, and processes affected by MC-LR and MC-RR, no fold change cutoff for DEGs was used. That being said, the discussion of our results is largely limited to functional enrichment analysis, which should mitigate the effects of including false positives.

3. Results

3.1. Cell viability

The LR1000 treatment group, and to a lesser degree, the LR100 and

RR1000 treatments displayed morphological changes consistent with cytotoxicity. The LR1000 and LR100 treatments demonstrated a dose-dependent reduction in survival using the XTT assay ($p < 0.05$).

3.2. Expression among MC treated cells

In all treatments, the majority of differentially expressed genes (DEGs) were up-regulated (Table 1). A much greater transcriptional response was observed with the LR1000 treatment relative to either of the other LR treatments. In contrast, a comparable number of DEGs was identified in the RR1000 and RR100 treatments. Few genes were identified in the RR10 treatment, suggesting that this concentration had little effect. Due to the low number of DEGs in the RR10 group, it was excluded from further analysis; however, complete lists of DEGs for all treatment groups can be found in Supplementary Table 1.

The magnitude of expression increased with treatment level for both the LR and RR treatments (Supplementary Table 1). This was most notable in the LR1000 group which had 84 genes with a > 2-fold change compared to 3 and 0 for the LR100 and LR10, respectively. The greatest fold change in the MC-RR groups was 1.7-fold in the RR1000 group.

Only eight DEGs overlapped among all three LR treatments (Fig. 1). The transcriptional response between the LR1000 and LR100 treatment groups was highly consistent with 59% of LR100 DEGs in common with LR1000. Five of the 10 most highly expressed genes in the LR1000 and LR100 gene lists were the same, with the top four being in the same relative order, further underscoring the consistency of the response. Despite observed cytotoxicity in the LR100 treatment group, relatively few DEGs were identified, suggesting greater variability among replicate exposure experiments. The gene expression response of the LR10 treatment group was markedly different from the other LR treatments displaying minimal overlap with either of the other LR treatments, with 10% and 8% of LR10 DEGs overlapping with LR1000 and LR100 respectively.

The RR1000 and RR100 treatment groups displayed moderate overlap (20%; 249/1255) (Fig. 1), and both overlapped to a similar extent with the LR1000 treatment (RR100 232/1255; RR1000 316/1279). Interestingly, the transcriptional response of LR10 appeared more similar to MC-RR groups than to either MC-LR treatment group (Supplementary Fig. 1; 13.6% and 16% of LR10 DEGs overlap with the RR100 and RR1000 groups respectively).

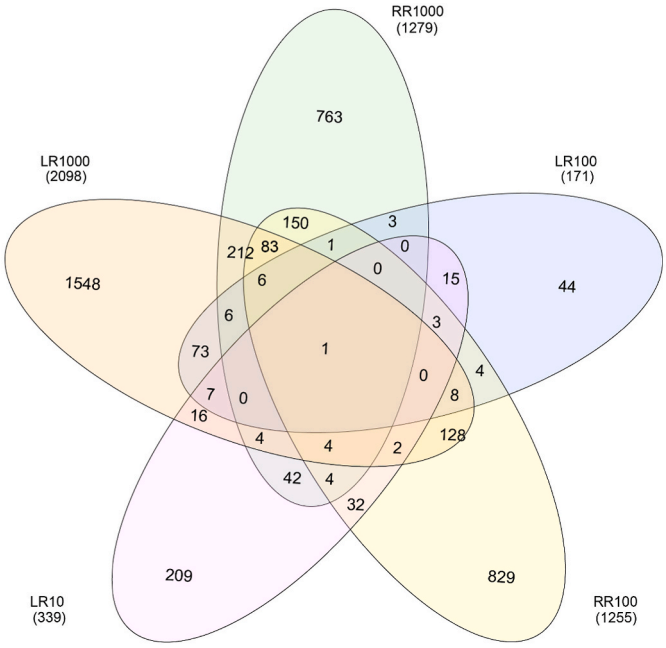

Fig. 1. Overlap of DEG among treatments.

In order to provide a more cohesive picture of the cellular response to MC-LR and MC-RR, enrichment analysis was conducted using both the DAVID for gene ontology (GO) terms (Table 2) and IPA for functional categories (Supplementary Table 2) and canonical pathways (Table 3). Enriched categories largely overlapped between MC-LR and MC-RR treatments and suggested the production of reactive oxygen species (ROS) is a key mediator of both MC-LR and MC-RR toxicity. With the exception of the enrichment of complement-associated categories by MC-RR, no strong evidence of congener-specific responses was observed.

4. Discussion

There has been a significant amount of research aimed at characterizing the drivers of MC-induced toxicity in hepatocytes. Much has focused on specific pathways or processes, resulting in a somewhat myopic view of the hepatocyte response to MCs and leading to conflicting interpretations. We employed whole transcriptome analysis with the goal of providing a comprehensive and non-targeted snapshot of early hepatocyte responses to MC exposures. Because harmful algal blooms (HABs) are generally composed of mixtures of MC congeners, identifying similarities and differences in cellular targets and effects may have some implications in estimating the full risk of MC mixtures. In order to identify potential differences among MC congeners, transcriptomic responses of hepatocytes exposed to either MC-LR or -RR congeners were evaluated.

To some degree, the comparisons of congeners were confounded with differences in the cytotoxicity of the LR and RR concentrations. The LR10 group may serve as a means of discriminating toxicity-related from congener-specific responses, as no cytotoxicity was observed with the treatment. Comparisons of enriched functional and canonical pathways, as well as overlaps in identified DEGs and principal component analysis, suggest that the LR10 treatment is similar to both the MC-LR and -RR treatments.

4.1. Complement system

Complement-related canonical pathways were identified as enriched in both DAVID and IPA analysis but not in MC-LR treatments (Tables 2 and 3). Some dose-dependence was suggested based on the number complement-related genes (27 genes in RR1000 group vs 14 in RR100; Supplementary Table 1). Twelve genes were identified in both treatments, suggesting a consistent response. Up-regulation of the complement system may be related to the acute phase response (APR), which was the most enriched canonical pathway in the MC-RR groups (Table 3); however, the APR was also enriched in MC-LR groups in the absence of complement-related genes, suggesting this may not be the case. Though generally associated with immunity and defense (Sarma and Ward, 2011), complement also plays important roles in the response to toxin-induced liver damage. Members of the complement system have been shown to protect hepatocytes from apoptosis during post-surgical liver regeneration (Markiewski et al., 2009). The protective functions of complement may partly explain the large difference in cytotoxic potential of MC-LR and MC-RR.

4.2. Extracellular exosomes

Extracellular exosome was among the most significantly enriched categories identified in DAVID analysis in the MC-RR treatment groups and was also observed, though less prominently, in the LR10 and LR1000 treatments. The consistency of exosome-related transcriptional response across treatment groups suggests it may be a common and important hepatocyte response to MC exposure. To our knowledge, the MC-dependent release of exosomes has not been previously reported, though exosome release has been linked to many of the key processes associated with MC toxicity, such as liver injury and oxidative stress

Table 2
Functional enrichment of MC-LR or MC-RR treated HepaRG cells. Functional enrichment of differentially expressed genes was conducted using DAVID. Results were trimmed to remove redundant entries (shaded rows). Values are Benjamini adjusted p-values.

Term	LR1000	LR100	LR10	RR1000	RR100
Phosphoprotein	1.8E-29	9.5E-03	2.0E-07	2.7E-17	2.1E-29
Acetylation	4.8E-20		2.6E-03	4.1E-27	2.4E-31
GO:0005515~protein binding	6.6E-10	7.4E-03		9.5E-03	5.6E-23
GO:0070062~extracellular exosome	3.1E-03		1.5E-04	6.4E-32	9.7E-22
GO:0005829~cytosol	4.3E-12	4.0E-02		1.9E-03	1.2E-13
Alternative splicing	8.8E-09		6.2E-04	1.0E-09	4.2E-11
Cytoplasm	1.5E-08		2.3E-03	4.8E-04	1.9E-08
Disease mutation	1.5E-02		8.4E-04	7.8E-09	2.9E-02
GO:0016020~membrane	1.4E-02			9.8E-08	2.7E-16
RNA binding related	4.7E-07			3.7E-03	1.4E-13
Ubl conjugation	7.9E-08			2.9E-02	4.6E-10
Endoplasmic reticulum	5.4E-07			3.6E-15	5.0E-05
mutagenesis site	1.0E-03			4.7E-02	3.9E-04
Nucleus	1.8E-04	4.2E-02			1.5E-03
Complement pathway related			1.4E-02	3.0E-14	7.2E-03
Nucleotide-binding	3.3E-06			1.7E-02	2.1E-02
cell-cell adhesion related				8.8E-06	1.4E-10
Isopeptide bond	8.6E-04				7.2E-10
GO:0005654~nucleoplasm	1.3E-07				6.5E-07
Endosome				2.3E-02	1.2E-06
Host-virus interaction				1.8E-02	1.5E-05
Golgi apparatus	3.6E-02				4.6E-05
Methylation	3.5E-02				2.8E-04
Transport				2.2E-03	3.0E-04
GO:0072562~blood microparticle				1.9E-13	2.8E-03
Coiled coil			3.8E-02		3.6E-02
Oxidoreductase	1.0E-05			2.2E-11	
Mitochondrion	1.4E-04			1.9E-10	
transit peptide:Mitochondrion	1.2E-02			3.1E-09	
GO:0005759~mitochondrial matrix	4.1E-03			4.5E-09	
NADP related	3.0E-02			9.0E-07	
hsa01100:Metabolic pathways	1.1E-02			1.0E-06	
Blood coagulation			3.6E-05	1.3E-05	
Microsome	5.2E-04			5.4E-05	
Acute phase			3.3E-02	4.8E-03	
ATP-binding	1.5E-03			3.2E-02	
Basic-leucine zipper domain	1.1E-05	2.1E-03			
Armadillo-type fold related					7.4E-06
Protein transport					4.5E-05
GO:0010951~negative regulation of endopeptidase activity				2.0E-06	
hsa01200:Carbon metabolism				5.2E-06	
GO:0005615~extracellular space				5.6E-06	
Fatty acid metabolism				8.0E-06	
Lipid metabolism				2.6E-05	

Stress response related	6.6E-05		
GO:0036499~PERK-mediated unfolded protein response	1.1E-04		
Apoptosis	1.6E-04		
Tubulin-related		1.5E-02	
GO:2000427~positive regulation of apoptotic cell clearance		3.7E-02	
GO:0001948~glycoprotein binding		4.4E-02	
IPR000837:Fos transforming protein	1.5E-03		
Postive regulation of transcription related	1.7E-03		
DNA-binding	8.4E-03		
GO:0044344~cellular response to fibroblast growth factor stimulus	1.9E-02		
GO:0051591~response to cAMP	2.7E-02		
GO:0009416~response to light stimulus	3.2E-02		
DNA-binding region:Basic motif	3.3E-02		

(Cho et al., 2018), lipotoxicity (Cazanave et al., 2011), ER stress and the UPR (Cazanave et al., 2011), and inflammation (Kakazu et al., 2016). The functional relevance of this is unclear, however, exosomes are known to act as pro-inflammatory extracellular signals, suggesting a potential mechanism for the immunostimulatory activity of MC. Alternatively, increases in exosome release following ER-stress is dependent on the several mediators of the unfolded protein response (UPR) (Kanemoto et al., 2016), suggesting exosomes may act to attenuate ER-stress (discussed below), potentially by offloading misfolded proteins.

4.3. Regulation of protein serine/threonine phosphatase related genes

The inhibition of PP activity is among the most well-characterized effects of MC, and congener-specific differences in PP targeting and inhibition have been previously reported (Honkanen et al., 1994; Pereira et al., 2013; Prickett and Brautigan, 2006). This is reflected in the transcriptional response as the term "phosphoprotein" was consistently among the most enriched terms across all treatments in DAVID analysis (Table 2). Little overlap in differentially expressed PP was observed between the LR and RR groups (Table 4). In MC-LR groups, a fairly consistent dose-dependent up-regulation of genes associated with PP1 and PP2, well known targets of MC-LR, was observed. In contrast, genes associated with five different PP family members were differentially expressed in MC-RR groups. The toxicological relevance of these observed differences is unclear given that PPs regulate numerous cellular functions, however, it is possible that the differential targeting of PP between MC congeners may play a role in differences in the toxicological response among congeners(Olsen et al., 2006). It is unclear if the differential expression of PP-related genes is a direct response to PP inhibition by MC or an indirect downstream effect. However, that these are very early responses (2 h) suggests these may be direct effects of MC/PP interactions.

4.4. Oxidative stress

In both congeners transcriptional responses consistently pointed to the production of ROS and subsequent oxidative stress. This is consistent with previous studies that observed increases in ROS in hepatocytes following exposure to several MC congeners (Cazenave et al., 2006; Kujbida et al., 2008; Weng et al., 2007). Pre-treatment with antioxidants effectively eliminates MC-LR-induced hepatocyte apoptosis, intrahepatic bleeding and serum markers of liver damage (Weng et al., 2007), suggesting ROS and oxidative stress are important factors in MC effects. In LR1000, LR100 and RR1000 treatments, the Nrf-2 canonical pathway was highly enriched (Table 3). Nrf-2 is a b-zip transcription factor that is activated following the production of ROS from diverse stimuli (Ma, 2013). Once activated, Nrf-2 binds to antioxidant response elements (ARE) and initiates a transcriptional response that includes up-regulation of genes involved in xenobiotic detoxification and antioxidant defense. Nrf-2 is considered a xenobiotic activated receptor (XAR) and its target genes overlap to a large degree with other members of this group that were also shown to be enriched across treatments, such as the AhR, FXR, and peroxisome proliferator-activated receptor (PPAR) (Ma, 2008). Nrf-2 target genes involved in maintaining intracellular GSH levels were up-regulated by both MC congeners (GCLC and GCLM, Supplementary Table 2); these proteins are known to detoxify MCs (Pflugmacher et al., 1998). Other Nrf-2 target genes involved in the oxidative stress response, such as the glutathione peroxidases (GPX) and several aldehyde dehydrogenases were also up-regulated across treatments, consistent with previous studies (Gehringer et al., 2004).

Though enrichment of the Nrf-2 oxidative response was observed in the RR1000 group, it was not among the top 30 enriched pathways, nor was it enriched in the RR100 or LR10 groups, suggesting some relationship to cytotoxicity. Interestingly, in both the RR100 and the LR10 groups, many cellular pathways associated with cytoskeletal structure were found to be enriched (Table 3). Disruption of cellular architecture is one of the most well characterized effects of MC exposure (Gehringer, 2004). The enrichment of cytoskeletal architecture-related pathways in the absence of evidence of strong oxidative stress response suggests that it either precedes or occurs at very low levels of oxidative stress. Further, the lack of cytotoxicity in these treatments suggests that changes in structural integrity are not directly responsible for cell death or occur very early in the cytotoxic pathway.

4.5. ER stress

The development of ER stress has previously been observed following MC exposure and has been suggested to be an alternative MC MOA (Menezes et al., 2013). In the current study, ER- and ER stress-related terms and transcripts were enriched by both congeners (Tables 2 and 3). ER stress results when the accumulation of newly translated proteins outpaces the folding capacity of the ER. This condition is toxic to cells and is mitigated via the UPR which is controlled by three transmembrane receptors, IRE-1, PERK, and activating transcription factor 6 (ATF6) that monitor the status of protein folding. MC-LR

Table 3
Enriched canonical pathways. DEGs of MC treated HepaRG cells were loaded into IPA. No fold change or significance filtering was conducted. Only the top 30 enriched pathways based on significance that overlapped with another treatment group are included. Values are -log Benjamini-Hochberg scores.

Ingenuity Canonical Pathways	LR1000	LR100	LR10	RR1000	RR100
Acute Phase Response Signaling	2.78		3.05	15	6.45
Germ Cell-Sertoli Cell Junction Signaling	3.36		6.3		1.94
Molecular Mechanisms of Cancer	2.58	1.59	1.99		
Sirtuin Signaling Pathway	2.27		1.53	4.11	
ERK/MAPK Signaling	2.2	2.39	1.48		
Glucocorticoid Receptor Signaling		1.69	1.59		2.88
14-3-3-mediated Signaling		1.51	2.21		1.79
NRF2-mediated Oxidative Stress Response	6.72	1.88			
Xenobiotic Metabolism Signaling	3.77			3.8	
IL-8 Signaling	2.78	1.59			
Aryl Hydrocarbon Receptor Signaling	2.78	1.83			
ILK Signaling	2.67	1.61			
Ethanol Degradation II	2.6			2.9	
LPS/IL-1 Mediated Inhibition of RXR Function	2.6			5.51	
Valine Degradation I	2.58			4.39	
IL-17A Signaling in Gastric Cells	2.58	1.88			
Oxidative Ethanol Degradation III	2.53			4.29	
Serotonin Degradation	2.43			2.41	
Putrescine Degradation III	2.34			2.99	
Complement System				7.16	2.88
LXR/RXR Activation			2.26	7.72	
Coagulation System				9.83	1.79
Remodeling of Epithelial Adherens Junctions			3.26		4.19
Phagosome Maturation			2.41		2.93
Clathrin-mediated Endocytosis Signaling			1.48		2.88
Actin Cytoskeleton Signaling			1.65		2.29
Sertoli Cell-Sertoli Cell Junction Signaling			3.43		2.28
Role of Tissue Factor in Cancer			2.93		2.28
Ephrin Receptor Signaling			1.57		2.09
Prolactin Signaling		1.83			2.09
Epithelial Adherens Junction Signaling			2.93		1.95
Endometrial Cancer Signaling			1.48		1.85
Role of Macrophages, Fibroblasts and Endothelial Cells in Rheumatoid Arthritis		1.48	1.74		

Table 4
Differentially expressed PP and PP-regulatory subunits.

Treatment	Gene Symbol	Gene Name
LR10	PPP1R13L	protein phosphatase 1 regulatory subunit 13 like
	PPP2R1A	protein phosphatase 2 scaffold subunit A alpha
LR100	PPP1R15A	protein phosphatase 1 regulatory subunit 15A
	PPP2R2D	protein phosphatase 2 regulatory subunit B delta
LR1000	PPP1CC	protein phosphatase 1 catalytic subunit gamma
	PPP1R10	protein phosphatase 1 regulatory subunit 10
	PPP1R15A	protein phosphatase 1 regulatory subunit 15A
	PPP1R15B	protein phosphatase 1 regulatory subunit 15B
	PPP2R1B	protein phosphatase 2 scaffold subunit A beta
	PPP2R2A	protein phosphatase 2 regulatory subunit B alpha
	PPP2R2D	protein phosphatase 2 regulatory subunit B delta
	PPP6R2	protein phosphatase 6 regulatory subunit 2
	PPM1D	protein phosphatase, Mg2+/Mn2+ dependent 1D
	PPTC7	PTC7 protein phosphatase homolog
RR100	PPP1CC	protein phosphatase 1 catalytic subunit gamma
	PPM1K	protein phosphatase, Mg2+/Mn2+ dependent 1K
	PPP1R2	protein phosphatase 1 regulatory inhibitor subunit 2
	PPP2CB	protein phosphatase 2 catalytic subunit beta
	PPP4R1	protein phosphatase 4 regulatory subunit 1
	PPP2CA	protein phosphatase 2 catalytic subunit alpha
	PPP6R3	protein phosphatase 6 regulatory subunit 3
	PDP1	Pyruvate dehydrogenase phosphatase catalytic subunit 1
RR1000	PPP4R2	protein phosphatase 4 regulatory subunit 2
	PPP5C	protein phosphatase 5 catalytic subunit
	PPP2R5A	protein phosphatase 2 regulatory subunit B alpha
	PPP2R1A	protein phosphatase 2 scaffold subunit A alpha
	SSH3	slingshot protein phosphatase 3
	PPP2CA	protein phosphatase 2 catalytic subunit alpha
	PPP6R3	protein phosphatase 6 regulatory subunit 3
	PDP1	Pyruvate dehydrogenase phosphatase catalytic subunit 1

has been shown to activate all three UPR response arms (Christen et al., 2013; Zhang et al., 2020), though the direct cause of MC-induced ER stress is unclear, ER stress is known to be induced by oxidative stress (Liu et al., 2018; Malhotra and Kaufman, 2007).

Gene expression changes detailed here, as well as those reported elsewhere, consistently point to the development of ER stress and activation of the UPR as significant determinants of cellular fate following MC exposure. There is conflicting evidence as to the consequence of MC-induced ER-stress, with some studies suggesting a pro-inflammatory response (Christen et al., 2013), while others a pro-apoptotic response (Menezes et al., 2013; Qin et al., 2010). This likely results from a significant degree of crosstalk among downstream pathways, overlap in pathway components, and the concurrent activation of multiple pathways downstream of different arms of the UPR. Consistent with this, evidence for both inflammatory and apoptotic responses was observed among treatments in the current study. Many inflammation-related canonical pathways were enriched across treatments (Table 3). Activation of the APR may provide a link between the immune response and ER-stress, as it has been shown to be via the ATF6 arm of the UPR (Zhang and Kaufman, 2008). Concurrent with inflammation, strong evidence of an apoptotic response was observed in the LR1000 and LR100 treatments. The PERK/CHOP arm of the UPR was highly enriched in the LR1000 treatment. CHOP initiates apoptosis through both the mitochondrial and death receptor pathways, as well as through the up-regulation of protein phosphatase 1 regulatory subunit 15A (PP1R15A/GADD34), which acts to intensify pro-apoptotic stimuli by re-initiating general transcription (Enyedi et al., 2010; Han et al., 2013; Marciniak et al., 2004; Yang et al., 2017). Up-regulation of CHOP target genes associated with both the mitochondrial (Phorbol-12-myristate-13-acetate-induced protein 1 (NOXA/PMAIP1), p53 up-regulated modulator of apoptosis (PUMA/BBC3)) and the death receptor (DR5) pathways, as well as GADD34, was observed in the LR1000 treatment. Further, ATF3, JUN and FOS, all components of the AP-1, a pro-apoptotic transcription factor activated downstream of ER stress, ROS production and MC-LR exposure, were among the most highly and consistently up-regulated genes in the cytotoxic LR treatments. The co-occurrence of indicators of inflammatory and apoptotic responses across treatments suggests that cells may simultaneously pursue multiple cellular programs and may help explain the conflicting evidence.

Ultimately, cellular fate is dependent on the severity and the duration of MC exposure and the differential activation of the three arms of the UPR. Several lines of evidence suggest that both the pro-inflammatory and -apoptotic programs converge on the stress activated c-Jun N-terminal kinase (JNK), suggesting it is the key determinant of cellular fate. MC-LR induces JNK activation in a time and dose-dependent manner (Sun et al., 2011) and JNK inhibition results in decreased responses associated with apoptosis, such as caspase activation, AP-1 binding, DNA fragmentation (Wei et al., 2008). Under cytotoxic conditions, JNK is activated as part of the ER-dependent apoptotic response via the IRE-1 pathway of the UPR (Urano et al., 2000). Additionally, JNK activation of CHOP, up-regulated via the PERK arm, results

in up-regulation of DR5 and the extrinsic apoptotic pathway (Guo et al., 2017). The transition between pro- and anti-apoptotic signaling is linked to the kinetics of JNK activation, with apoptosis associated with sustained JNK activation and cell survival with transient activation. This is regulated via the pro-inflammatory factor NF-κβ which inhibits sustained JNK activation resulting in increased survival (Tang et al., 2002). Activation of NF-κβ has been demonstrated downstream of MC-LR induced ER stress concomitant with up-regulation of pro-inflammatory factors such as INF- α, as well as TNF-α, which is also associated with apoptosis (Christen et al., 2013; Zhang et al., 2013). Together, this suggests a mechanism whereby MC exposures promote ROS production and oxidative stress leading to ER stress and activation of JNK and NF-kB downstream of the UPR (Fig. 2). Under non-cytotoxic conditions, an inflammatory and pro-survival response is favored via NF-κβ inhibition of sustained JNK activation and up-regulation of pro-inflammatory genes. However, under conditions where ER stress cannot be mitigated, apoptosis is induced via IRE-1 activation of JNK through MAPK and p38 signaling and through PERK/IRE-1/ATF-6 up-regulation of CHOP and subsequent activation of apoptotic pathways. The suggestion of NF-kB/JNK as a pro/anti-apoptotic switch is supported by evidence demonstrating that NF-kB activation and DNA binding is dependent on MC concentration (Chen et al., 2016; Zhang et al., 2013).

5. Conclusions

Using a non-targeted transcriptional approach, we have provided a holistic picture of the early hepatocyte response to MC-LR and -RR exposure. Many of the enriched processes and pathways, as well as the specific DEGs have been previously reported, underscoring the validity of our approach and interpretation. We demonstrate differences in the transcriptional profiles of PP-related genes between MC congeners, which may underlie congener-specific effects. Through functional enrichment analysis we have identified several previously unreported effects and congener differences. Among the most striking is the enrichment of complement-related genes in MC-RR treatments, but not MC-LR treatments, which may partially explain differences in toxicity between congeners. Genes related to extracellular exosomes were highly enriched by both congeners, suggesting a previously unreported pathway of MC-dependent extracellular signaling. For both congeners, the majority of evidence either directly or indirectly points to the induction of oxidative stress. We propose a model of MC toxicity that begins with oxidative stress and leads to ER stress and the initiation of the UPR. All three arms of the UPR converge on the activation of JNK which, depending on the severity of the MC toxicity, ultimately determines cellular fate through its interactions with NF-κB. Though this model has not yet been tested, it is supported by previous studies and may explain conflicting interpretations of the hepatocyte response to MC exposure.

Ethics statement

No human or animal subjects were used for this study.

Funding

This research received no external funding

Disclaimer

The views expressed in this article are those of the authors and do not necessarily reflect the views or policies of the U.S. Environmental Protection Agency. Any mention of trade names, products, or services does not imply an endorsement by the U.S. Government or the U.S. Environmental Protection Agency (EPA). The EPA does not endorse any commercial products, services, or enterprises.

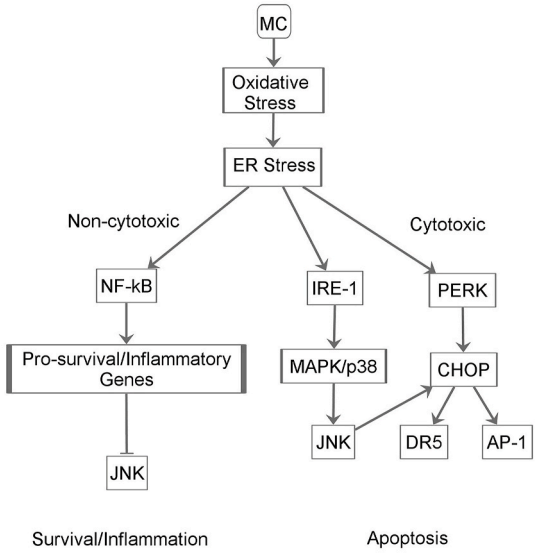

Fig. 2. A model of the hepatocyte response to MC exposure. MC initiate the production of ROS, resulting in the accumulation of mis and non-folded proteins in the lumen of the ER. Accumulation of these proteins results in ER stress and initiation of all three arms of the UPR. Depending on the severity of the MC exposure cellular fate is ultimately decided by the kinetics of JNK activation. Sustained JNK activation leads to PERK/CHOP mediated apoptosis via both the mitochondrial and DR pathway. Lower levels of MC exposure result in the upregulation of NF-κB which initiates a pro-survival/inflammatory response that inhibits sustained JNK activation.

CRediT authorship contribution statement

Adam D. Biales: Conceptualization, Methodology, Formal analysis, Writing - original draft, Writing - review & editing. **David C. Bencic:** Conceptualization, Methodology, Investigation, Writing - review & editing. **Robert W. Flick:** Conceptualization, Methodology, Investigation, Writing - review & editing. **Armah Delacruz:** Methodology, Investigation, Writing - review & editing. **Denise A. Gordon:** Investigation, Writing - review & editing. **Weichun Huang:** Conceptualization, Data curation, Methodology, Formal analysis, Writing - original draft, Writing - review & editing.

Declaration of competing interest

The authors declare that they have no known competing financial interests or personal relationships that could have appeared to influence the work reported in this paper.

Acknowledgement

The RTSF Genomics Core at Michigan State University provided sequencing services for this work.

Appendix A. Supplementary data

Supplementary data to this article can be found online at https://doi.org/10.1016/j.toxcx.2020.100060.

References

Alverca, E., Andrade, M., Dias, E., Sam Bento, F., Batoreu, M.C., Jordan, P., Silva, M.J., Pereira, P., 2009. Morphological and ultrastructural effects of microcystin-LR from Microcystis aeruginosa extract on a kidney cell line. Toxicon : Off. J. Int. Soc. Toxinol. 54, 283–294.

Bates, D., Machler, M., Bolker, B., Walker, S., 2015. Fitting linear mixed-effects models using lme4. J. Stat. Software 67, 1–48.

Batista, T., de Sousa, G., Suput, J.S., Rahmani, R., Suput, D., 2003. Microcystin-LR causes the collapse of actin filaments in primary human hepatocytes. Aquat. Toxicol. 65, 85–91.
Bouaicha, N., Miles, C.O., Beach, D.G., Labidi, Z., Djabri, A., Benayache, N.Y., Nguyen-Quang, T., 2019. Structural diversity, characterization and toxicology of microcystins. Toxins (Basel) 11.
Brown, J., Pirrung, M., McCue, L.A., 2017. FQC Dashboard: integrates FastQC results into a web-based, interactive, and extensible FASTQ quality control tool. Bioinformatics.
Cazanave, S.C., Mott, J.L., Bronk, S.F., Werneburg, N.W., Fingas, C.D., Meng, X.W., Finnberg, N., El-Deiry, W.S., Kaufmann, S.H., Gores, G.J., 2011. Death receptor 5 signaling promotes hepatocyte lipoapoptosis. J. Biol. Chem. 286, 39336–39348.
Cazenave, J., Bistoni Mde, L., Pesce, S.F., Wunderlin, D.A., 2006. Differential detoxification and antioxidant response in diverse organs of Corydoras paleatus experimentally exposed to microcystin-RR. Aquat. Toxicol. 76, 1–12.
Chen, L., Li, S., Guo, X., Xie, P., Chen, J., 2016. The role of GSH in microcystin-induced apoptosis in rat liver: involvement of oxidative stress and NF-kappaB. Environ. Toxicol. 31, 552–560.
Chen, T., Cui, J., Liang, Y., Xin, X., Owen Young, D., Chen, C., Shen, P., 2006. Identification of human liver mitochondrial aldehyde dehydrogenase as a potential target for microcystin-LR. Toxicology 220, 71–80.
Cho, Y.E., Seo, W., Kim, D.K., Moon, P.G., Kim, S.H., Lee, B.H., Song, B.J., Baek, M.C., 2018. Exogenous exosomes from mice with acetaminophen-induced liver injury promote toxicity in the recipient hepatocytes and mice. Sci. Rep. 8, 16070.
Christen, V., Meili, N., Fent, K., 2013. Microcystin-LR induces endoplasmatic reticulum stress and leads to induction of NFkappaB, interferon-alpha, and tumor necrosis factor-alpha. Environ. Sci. Technol. 47, 3378–3385.
Diez-Quijada, L., Puerto, M., Gutierrez-Praena, D., Llana-Ruiz-Cabello, M., Jos, A., Camean, A.M., 2019. Microcystin-RR: occurrence, content in water and food and toxicological studies. A review. Environ. Res. 168, 467–489.
Dyble, J., Fahnenstiel, G.L., Litaker, R.W., Millie, D.F., Tester, P.A., 2008. Microcystin concentrations and genetic diversity of Microcystis in the lower Great Lakes. Environ. Toxicol. 23, 507–516.
Enyedi, B., Varnai, P., Geiszt, M., 2010. Redox state of the endoplasmic reticulum is controlled by Ero1L-alpha and intraluminal calcium. Antioxidants Redox Signal. 13, 721–729.
Evans, T.G., 2015. Considerations for the use of transcriptomics in identifying the 'genes that matter' for environmental adaptation. J. Exp. Biol. 218, 1925–1935.
Fischer, A., Hoeger, S.J., Stemmer, K., Feurstein, D.J., Knobeloch, D., Nussler, A., Dietrich, D.R., 2010. The role of organic anion transporting polypeptides (OATPs/SLCOs) in the toxicity of different microcystin congeners in vitro: a comparison of primary human hepatocytes and OATP-transfected HEK293 cells. Toxicol. Appl. Pharmacol. 245, 9–20.
Fischer, W.J., Altheimer, S., Cattori, V., Meier, P.J., Dietrich, D.R., Hagenbuch, B., 2005. Organic anion transporting polypeptides expressed in liver and brain mediate uptake of microcystin. Toxicol. Appl. Pharmacol. 203, 257–263.
Frankish, A., Uszczynska, B., Ritchie, G.R., Gonzalez, J.M., Pervouchine, D., Petryszak, R., Mudge, J.M., Fonseca, N., Brazma, A., Guigo, R., Harrow, J., 2015. Comparison of GENCODE and RefSeq gene annotation and the impact of reference geneset on variant effect prediction. BMC Genom. 16 (Suppl. 8), S2.
Gehringer, M.M., 2004. Microcystin-LR and okadaic acid-induced cellular effects: a dualistic response. FEBS Lett. 557, 1–8.
Gehringer, M.M., Shephard, E.G., Downing, T.G., Wiegand, C., Neilan, B.A., 2004. An investigation into the detoxification of microcystin-LR by the glutathione pathway in Balb/c mice. Int. J. Biochem. Cell Biol. 36, 931–941.
Graham, J.L., Loftin, K.A., Meyer, M.T., Ziegler, A.C., 2010. Cyanotoxin mixtures and taste-and-odor compounds in cyanobacterial blooms from the Midwestern United States. Environ. Sci. Technol. 44, 7361–7368.
Guo, X., Meng, Y., Sheng, X., Guan, Y., Zhang, F., Han, Z., Kang, Y., Tai, G., Zhou, Y., Cheng, H., 2017. Tunicamycin enhances human colon cancer cells to TRAIL-induced apoptosis by JNK-CHOP-mediated DR5 upregulation and the inhibition of the EGFR pathway. Anti Canc. Drugs 28, 66–74.
Gupta, N., Pant, S.C., Vijayaraghavan, R., Rao, P.V., 2003. Comparative toxicity evaluation of cyanobacterial cyclic peptide toxin microcystin variants (LR, RR, YR) in mice. Toxicology 188, 285–296.
Han, J., Back, S.H., Hur, J., Lin, Y.H., Gildersleeve, R., Shan, J., Yuan, C.L., Krokowski, D., Wang, S., Hatzoglou, M., Kilberg, M.S., Sartor, M.A., Kaufman, R.J., 2013. ER-stress-induced transcriptional regulation increases protein synthesis leading to cell death. Nat. Cell Biol. 15, 481–490.
Harke, M.J., Steffen, M.M., Gobler, C.J., Otten, T.G., Wilhelm, S.W., Wood, S.A., Paerl, H. W., 2016. A review of the global ecology, genomics, and biogeography of the toxic cyanobacterium. Microcystis spp. Harmful algae 54, 4–20.
Harrow, J., Frankish, A., Gonzalez, J.M., Tapanari, E., Diekhans, M., Kokocinski, F., Aken, B.L., Barrell, D., Zadissa, A., Searle, S., Barnes, I., Bignell, A., Boychenko, V., Hunt, T., Kay, M., Mukherjee, G., Rajan, J., Despacio-Reyes, G., Saunders, G., Steward, C., Harte, R., Lin, M., Howald, C., Tanzer, A., Derrien, T., Chrast, J., Walters, N., Balasubramanian, S., Pei, B., Tress, M., Rodriguez, J.M., Ezkurdia, I., van Baren, J., Brent, M., Haussler, D., Kellis, M., Valencia, A., Reymond, A., Gerstein, M., Guigo, R., Hubbard, T.J., 2012. GENCODE: the reference human genome annotation for the ENCODE Project. Genome Res. 22, 1760–1774.
Higuchi, Y., Kawai, K., Yamazaki, H., Nakamura, M., Bree, F., Guguen-Guillouzo, C., Suemizu, H., 2014. The human hepatic cell line HepaRG as a possible cell source for the generation of humanized liver TK-NOG mice. Xenobiotica 44, 146–153.
Hoeger, S.J., Schmid, D., Blom, J.F., Ernst, B., Dietrich, D.R., 2007. Analytical and functional characterization of microcystins [Asp3]MC-RR and [Asp3,Dhb7]MC-RR: consequences for risk assessment? Environ. Sci. Technol. 41, 2609–2616.
Honkanen, R.E., Codispoti, B.A., Tse, K., Boynton, A.L., Honkanan, R.E., 1994. Characterization of natural toxins with inhibitory activity against serine/threonine protein phosphatases. Toxicon : Off. J. Int. Soc. Toxinol. 32, 339–350.
Huang da, W., Sherman, B.T., Lempicki, R.A., 2009. Bioinformatics enrichment tools: paths toward the comprehensive functional analysis of large gene lists. Nucleic Acids Res. 37, 1–13.
Huang, W., Umbach, D.M., Vincent Jordan, N., Abell, A.N., Johnson, G.L., Li, L., 2011. Efficiently identifying genome-wide changes with next-generation sequencing data. Nucleic Acids Res. 39, e130.
Josse, R., Aninat, C., Glaise, D., Dumont, J., Fessard, V., Morel, F., Poul, J.M., Guguen-Guillouzo, C., Guillouzo, A., 2008. Long-term functional stability of human HepaRG hepatocytes and use for chronic toxicity and genotoxicity studies. Drug Metabol. Dispos.: Biol. Fate. Chem. 36, 1111–1118.
Kakazu, E., Mauer, A.S., Yin, M., Malhi, H., 2016. Hepatocytes release ceramide-enriched pro-inflammatory extracellular vesicles in an IRE1alpha-dependent manner. J. Lipid Res. 57, 233–245.
Kanemoto, S., Nitani, R., Murakami, T., Kaneko, M., Asada, R., Matsuhisa, K., Saito, A., Imaizumi, K., 2016. Multivesicular body formation enhancement and exosome release during endoplasmic reticulum stress. Biochem. Biophys. Res. Commun. 480, 166–172.
Kujbida, P., Hatanaka, E., Campa, A., Curi, R., Poliselli Farsky, S.H., Pinto, E., 2008. Analysis of chemokines and reactive oxygen species formation by rat and human neutrophils induced by microcystin-LA, -YR and -LR. Toxicon : Off. J. Int. Soc. Toxinol. 51, 1274–1280.
Kuznetsova, A., Brockhoff, P.B., Christensen, R.H.B., 2017. lmerTest package: tests in linear mixed effects models. J. Stat. Software 82, 1–26.
Leek, J.W., Johnson, W., Parker, H., Fertig, E., Jaffe, A., Storey, J., Zhang, Y., Torres, L., 2018. Sva: surrogate variable analysis. R package version 3.29.1.
Li, H., Durbin, R., 2009. Fast and accurate short read alignment with Burrows-Wheeler transform. Bioinformatics 25, 1754–1760.
Lin, H., Liu, W., Zeng, H., Pu, C., Zhang, R., Qiu, Z., Chen, J.A., Wang, L., Tan, Y., Zheng, C., Yang, X., Tian, Y., Huang, Y., Luo, J., Luo, Y., Feng, X., Xiao, G., Feng, L., Li, H., Wang, F., Yuan, C., Wang, J., Zhou, Z., Wei, T., Zuo, Y., Wu, L., He, L., Guo, Y., Shu, W., 2016. Determination of environmental exposure to microcystin and aflatoxin as a risk for renal function based on 5493 rural people in Southwest China. Environ. Sci. Technol. 50, 5346–5356.
Liu, H., Zhang, X., Zhang, S., Huang, H., Wu, J., Wang, Y., Yuan, L., Liu, C., Zeng, X., Cheng, X., Zhuang, D., Zhang, H., 2018. Oxidative stress mediates microcystin-LR-induced endoplasmic reticulum stress and autophagy in KK-1 cells and C57BL/6 mice ovaries. Front. Physiol. 9, 1058.
Ma, Q., 2008. Xenobiotic-activated receptors: from transcription to drug metabolism to disease. Chem. Res. Toxicol. 21, 1651–1671.
Ma, Q., 2013. Role of nrf2 in oxidative stress and toxicity. Annu. Rev. Pharmacol. Toxicol. 53, 401–426.
Malhotra, J.D., Kaufman, R.J., 2007. Endoplasmic reticulum stress and oxidative stress: a vicious cycle or a double-edged sword? Antioxidants Redox Signal. 9, 2277–2293.
Marciniak, S.J., Yun, C.Y., Oyadomari, S., Novoa, I., Zhang, Y., Jungreis, R., Nagata, K., Harding, H.P., Ron, D., 2004. CHOP induces death by promoting protein synthesis and oxidation in the stressed endoplasmic reticulum. Genes Dev. 18, 3066–3077.
Markiewski, M.M., DeAngelis, R.A., Strey, C.W., Foukas, P.G., Gerard, C., Gerard, N., Wetsel, R.A., Lambris, J.D., 2009. The regulation of liver cell survival by complement. J. Immunol. 182, 5412–5418.
Massey, I.Y., Yang, F., Ding, Z., Yang, S., Guo, J., Tezi, C., Al-Osman, M., Kamegni, R.B., Zeng, W., 2018. Exposure routes and health effects of microcystins on animals and humans: a mini-review. Toxicon : Off. J. Int. Soc. Toxinol. 151, 156–162.
Menezes, C., Alverca, E., Dias, E., Sam-Bento, F., Pereira, P., 2013. Involvement of endoplasmic reticulum and autophagy in microcystin-LR toxicity in Vero-E6 and HepG2 cell lines. Toxicol. Vitro 27, 138–148.
Olsen, J.V., Blagoev, B., Gnad, F., Macek, B., Kumar, C., Mortensen, P., Mann, M., 2006. Global, in vivo, and site-specific phosphorylation dynamics in signaling networks. Cell 127, 635–648.
Pereira, S.R., Vasconcelos, V.M., Antunes, A., 2013. Computational study of the covalent bonding of microcystins to cysteine residues–a reaction involved in the inhibition of the PPP family of protein phosphatases. FEBS J. 280, 674–680.
Pflugmacher, S., Wiegand, C., Oberemm, A., Beattie, K.A., Krause, E., Codd, G.A., Steinberg, C.E., 1998. Identification of an enzymatically formed glutathione conjugate of the cyanobacterial hepatotoxin microcystin-LR: the first step of detoxication. Biochim. Biophys. Acta 1425, 527–533.
Prickett, T.D., Brautigan, D.L., 2006. The alpha4 regulatory subunit exerts opposing allosteric effects on protein phosphatases PP6 and PP2A. J. Biol. Chem. 281, 30503–30511.
Qin, W., Xu, L., Zhang, X., Wang, Y., Meng, X., Miao, A., Yang, L., 2010. Endoplasmic reticulum stress in murine liver and kidney exposed to microcystin-LR. Toxicon : Off. J. Int. Soc. Toxinol. 56, 1334–1341.
Runnegar, M., Berndt, N., Kaplowitz, N., 1995. Microcystin uptake and inhibition of protein phosphatases: effects of chemoprotectants and self-inhibition in relation to known hepatic transporters. Toxicol. Appl. Pharmacol. 134, 264–272.
Sarma, J.V., Ward, P.A., 2011. The complement system. Cell Tissue Res. 343, 227–235.
St Laurent, G., Shtokalo, D., Tackett, M.R., Yang, Z., Vyatkin, Y., Milos, P.M., Seilheimer, B., McCaffrey, T.A., Kapranov, P., 2013. On the importance of small changes in RNA expression. Methods 63, 18–24.
Sun, Y., Meng, G.M., Guo, Z.L., Xu, L.H., 2011. Regulation of heat shock protein 27 phosphorylation during microcystin-LR-induced cytoskeletal reorganization in a human liver cell line. Toxicol. Lett. 207, 270–277.

Szabo, M., Veres, Z., Baranyai, Z., Jakab, F., Jemnitz, K., 2013. Comparison of human hepatoma HepaRG cells with human and rat hepatocytes in uptake transport assays in order to predict a risk of drug induced hepatotoxicity. PloS One 8, e59432.
Takumi, S., Komatsu, M., Furukawa, T., Ikeda, R., Sumizawa, T., Akenaga, H., Maeda, Y., Aoyama, K., Arizono, K., Ando, S., Takeuchi, T., 2010. p53 Plays an important role in cell fate determination after exposure to microcystin-LR. Environ. Health Perspect. 118, 1292–1298.
Tang, F., Tang, G., Xiang, J., Dai, Q., Rosner, M.R., Lin, A., 2002. The absence of NF-kappaB-mediated inhibition of c-Jun N-terminal kinase activation contributes to tumor necrosis factor alpha-induced apoptosis. Mol. Cell Biol. 22, 8571–8579.
Team, R.C., 2017. R: A Language and Environment for Statistical Computing. R Foundation for Statistical Computing, Vienna, Austria.
Urano, F., Wang, X., Bertolotti, A., Zhang, Y., Chung, P., Harding, H.P., Ron, D., 2000. Coupling of stress in the ER to activation of JNK protein kinases by transmembrane protein kinase IRE1. Science 287, 664–666.
Vesterkvist, P.S., Meriluoto, J.A., 2003. Interaction between microcystins of different hydrophobicities and lipid monolayers. Toxicon : Off. J. Int. Soc. Toxinol. 41, 349–355.
Wei, Y., Weng, D., Li, F., Zou, X., Young, D.O., Ji, J., Shen, P., 2008. Involvement of JNK regulation in oxidative stress-mediated murine liver injury by microcystin-LR. Apoptosis : Int. J. Program. Cell Death 13, 1031–1042.
Weng, D., Lu, Y., Wei, Y., Liu, Y., Shen, P., 2007. The role of ROS in microcystin-LR-induced hepatocyte apoptosis and liver injury in mice. Toxicology 232, 15–23.
Yang, Y., Liu, L., Naik, I., Braunstein, Z., Zhong, J., Ren, B., 2017. Transcription factor C/EBP homologous protein in health and diseases. Front. Immunol. 8, 1612.
Yoshida, T., Makita, Y., Tsutsumi, T., Nagata, S., Tashiro, F., Yoshida, F., Sekijima, M., Tamura, S., Harada, T., Maita, K., Ueno, Y., 1998. Immunohistochemical localization of microcystin-LR in the liver of mice: a study on the pathogenesis of microcystin-LR-induced hepatotoxicity. Toxicol. Pathol. 26, 411–418.
Yoshizawa, S., Matsushima, R., Watanabe, M.F., Harada, K., Ichihara, A., Carmichael, W. W., Fujiki, H., 1990. Inhibition of protein phosphatases by microcystins and nodularin associated with hepatotoxicity. J. Canc. Res. Clin. Oncol. 116, 609–614.
Zhang, D., Lin, W., Liu, Y., Guo, H., Wang, L., Yang, L., Li, L., Li, D., Tang, R., 2020. Chronic microcystin-LR exposure induces abnormal lipid metabolism via endoplasmic reticulum stress in male zebrafish. Toxins (Basel) 12.
Zhang, J., Chen, J., Xia, Z., 2013. Microcystin-LR exhibits immunomodulatory role in mouse primary hepatocytes through activation of the NF-kappaB and MAPK signaling pathways. Toxicol. Sci. : Off. J. Soc. Toxicol. 136, 86–96.
Zhang, K., Kaufman, R.J., 2008. From endoplasmic-reticulum stress to the inflammatory response. Nature 454, 455–462.